

Leveraging Intrinsic Gradient Information for Machine Learning Model Training

Chris McDonagh¹, Xi Chen¹

¹Department of Computer Science, University of Bath, Bath, BA2 7PB, UK
{cm2042, xc841}@bath.ac.uk,

Abstract

Designing models that produce accurate predictions is the fundamental objective of machine learning. This work presents methods demonstrating that when the derivatives of target variables with respect to inputs can be extracted from processes of interest, they can be leveraged to improve the accuracy of differentiable machine learning models. Four key ideas are explored: (1) Improving the predictive accuracy of linear regression models and feed-forward neural networks (NNs); (2) Using the difference between the performance of feedforward NNs trained with and without gradient information to tune NN complexity (in the form of hidden node number); (3) Using gradient information to regularise linear regression; and (4) Using gradient information to improve generative image models. Across this variety of applications, gradient information is shown to enhance each predictive model, demonstrating its value for a variety of applications.

1 Introduction

Designing models that can accurately make predictions is the fundamental objective of machine learning. It is well understood in machine learning that model parameters can be optimised using a training data set comprised of inputs and output labels. This paper aims to highlight to practitioners that more information to train models may be available by way of gradient information.

The idea has been explored in [Brehmer *et al.*, 2020], in which the authors investigate latent variable estimation problems in computer simulator based systems and demonstrate how the ‘joint score’ from stochastic simulators can be used to improve the accuracy of neural network conditional density estimators for Bayesian inference. The ‘joint score’ refers to the derivative of the joint probability $\nabla_{\theta_0} p(\mathbf{x}, \mathbf{z}|\theta_0) = t(\mathbf{x}, \mathbf{z}|\theta)$ where \mathbf{z} refers to the latent path that an output \mathbf{x} takes through a simulator and θ represents the corresponding variables. This gradient information can be used in conjunction with a classification method referred to as the Likelihood Ratio Trick (LRT) (see [Tran *et al.*, 2017], [Gutmann *et al.*, 2018] and [Brehmer *et al.*, 2020] for more details)

to improve the estimation of unknown parameter probability densities using neural networks. The LRT is mainly used for likelihood-free problems where the likelihood can not be explicitly defined (sometimes even intractable) and therefore makes Bayesian inference challenging. Recently, [Brehmer *et al.*, 2020] present the first work the authors are aware of that demonstrate how gradient information can be used to improve machine learning model fit.

Extending this insight, this work generalises the idea and provides practical methodologies that can be used to leverage gradient information. The supervised learning problem along with the logic underpinning the value of gradient information for neural networks is presented formally in Section 3. Following these results, Section 4 lays the foundations for using gradient information to tune neural network complexity, proposing an application in genetic hyper-parameter optimisation pipeline. Section 5 presents a novel linear regression regulariser that uses gradient information to outperform ridge regression. Finally, Section 6 demonstrates how gradients can be used to improve generative image models. The main contributions of this work are as follows:

- Improved unknown parameter estimation: Methods that leverage gradient information to train surrogate models and perform more accurate latent parameter estimation using MLE are presented in Section 3.
- Tuning neural network complexity with delta-min metric: Section 4 presents a novel metric that can be utilised in a hyper parameter optimisation pipeline that provides an indicator of an upper bound to neural network complexity.
- Ridge-Gradients regularisation: A novel regularisation method for linear regression that outperforms conventional ridge regularisation over varying training sample sizes by utilising gradient information is presented in Section 5.
- Improving generative model prediction: Section 6 presents a novel GAN training algorithm that utilises gradient information to train an improved generator.

2 Training neural networks with gradients

Consider a real-world process P that takes inputs X to produce outputs Z :

$$\mathbf{Z} = P(\mathbf{X}). \quad (1)$$

Supervised learning aims to design and train a model to emulate this process \hat{P} :

$$\hat{\mathbf{z}} = \hat{P}_\varphi(\mathbf{x}). \quad (2)$$

This requires collecting data on the independent variable $\mathbf{z} \subseteq \mathbf{Z}$ and dependent variables $\mathbf{x} \subseteq \mathbf{X}$ for which data exist. The parameters of the selected model can then be trained using training data with N samples $\{\mathbf{x}_i, \mathbf{z}_i\}_{i=1}^N$.

The primary contribution of this work is to present that if the derivatives of process outputs with respect to their inputs $\frac{\delta \mathbf{z}_i}{\delta \mathbf{x}_i}$ can be extracted, expanding the training data set to $\{\mathbf{x}_i, \mathbf{z}_i, \frac{\delta \mathbf{z}_i}{\delta \mathbf{x}_i}\}_{i=1}^N$ then they can be useful for training neural networks. These derivatives of process outputs are referred to throughout this paper as 'gradient information'.

Why is gradient information valuable?

First consider the conventional training mechanism of a neural network, presented below:

$$\theta_i^+ = \theta_i - \eta \frac{\delta E}{\delta \theta_i} \quad (3)$$

where θ_i is the i th parameter in network of given complexity and η represents a learning rate. E represents some error function which, using the training data $\{\mathbf{x}_i, \mathbf{z}_i\}_{i=1}^N$, defines how 'good' a model is. Neural networks learn to emulate P via these parameter updates, which directly target the loss function E .

As a neural network is a differentiable with respect to its inputs, $\frac{\delta \hat{\mathbf{z}}}{\delta \mathbf{x}}$ can be calculated. Practitioners can therefore impose that not only should a network's outputs emulate target variables, but also that the derivative of network outputs with respect to inputs $\frac{\delta \hat{\mathbf{z}}}{\delta \mathbf{x}}$ should match the derivative of true outputs with respect to inputs $\frac{\delta \mathbf{z}_i}{\delta \mathbf{x}_i}$.

To implement this, an additional error function is required, E_{grad} , that evaluates the accuracy of the neural network's derivatives compared to the true process derivatives. The parameter update mechanism therefore becomes:

$$\theta_i^+ = \theta_i - \alpha \eta \frac{\delta E}{\delta \theta_i} - ((1 - \alpha) \eta \frac{\delta E_{grad}}{\delta \theta_i}) \quad (4)$$

where α represents a weighting to attached to each loss function. This can be critical when the magnitude of the target loss function E and gradient loss function E_{grad} differ materially.

When trained with gradient information, equation 4 shows that the absolute magnitude of each parameter update must be larger than when gradient information is not included¹. Under

¹Note that a parameter update can be smaller when gradient information is included as the error the results from gradient fitting can effectively offset the error that results from target fitting, however the absolute error must be larger, despite their respective signs causing offsetting.

the assumption that on average, a parameter update is beneficial for a model, which implies that model training generally is sensible (e.g. over-fitting is avoided), then the relative increase in the magnitude of parameter updates that result from training a network with gradient information represents its marginal value.

To illustrate this, consider the following toy function:

$$\mathbf{Z} = 2\mathbf{X}^2 + \epsilon \quad (5)$$

where $\epsilon \sim N(0, 1)$. To emulate this function, we design a feed-forward neural network of sufficient complexity to avoid under fitting. N samples of synthetic data, including gradient information, are then generated from the toy function and used to train the neural network. Figure 1 illustrates this process, showing how the average update to neural network parameter values is larger each epoch when the network is trained with gradients. This in turn helps the gradient trained network outperform its conventionally trained counterpart.

A key feature of the value of gradient information is that it reduces as the training sample size N increases. This results when the marginal training data sample improves model fit (i.e. when model hyper-parameters are properly tuned). To illustrate this, consider the following: A sensible choice for the type E_{grad} loss function is mean-squared error as gradients are typically continuous (even when target variables are discrete).

$$E_{grad} = \left(\frac{\delta \mathbf{z}}{\delta \mathbf{x}} - \frac{\delta \hat{\mathbf{z}}}{\delta \mathbf{x}} \right)^2 \quad (6)$$

Under the assumption that as N increases the average predictions of $\hat{P}_\varphi(\mathbf{x})$ results in a yields lower error, then $\frac{\delta \hat{\mathbf{z}}}{\delta \mathbf{x}}$ more closely emulates $\frac{\delta \mathbf{z}}{\delta \mathbf{x}}$ and therefore the marginal value of gradient information, quantified by the magnitude of the parameter updates, falls.

This is shown in Figure 1. With a relatively small training sample size of 250, the persistence in the relatively larger parameter updates per epoch for the gradient trained network drives out performance. In contrast, with the relatively larger training sample size of 1000, the delta of parameter changes per epoch converges sooner, due to the loss defined in equation 6 reducing as a result of increased training sample size causing improved gradient fitting.

3 Latent parameter estimation

A application of methods that leverage gradient information for probabilistic machine learning is statistical estimation of unknown parameters in social and physical systems. Techniques to estimate parameters such as Approximate Bayesian Computation (ABC) (see [Rubin, 1984] for key ideas and [Blum *et al.*, 2013] for a detailed review and comparison of various ABC methods) and Neural Density Estimation (NDE) (see [Thomas *et al.*, 2016], [Papamakarios and Murray, 2016] and [van den Oord *et al.*, 2016] for examples) can require several thousand evaluations of computer simulators designed by domain experts to emulate a process of interest. If such simulators are computationally expensive to evaluate (for example the black-oil model discussed in [Casciano *et al.*, 2015]

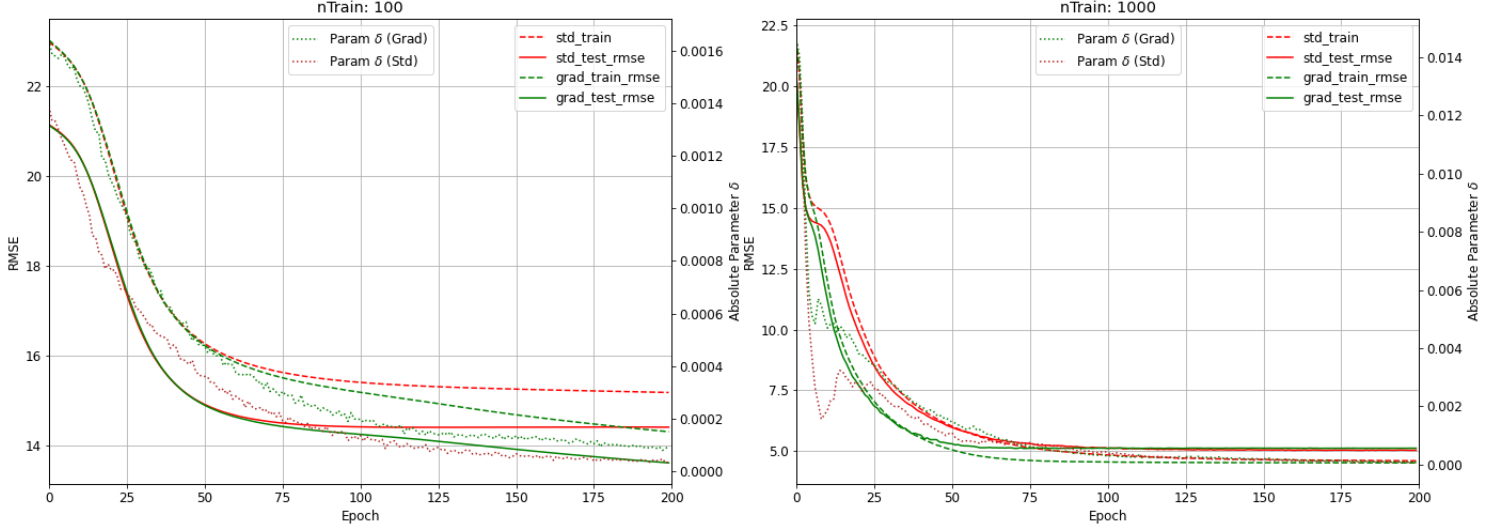


Figure 1: Train and test RMSE of neural networks trained with and without gradients. Absolute change in parameters is shown in right axes. **Left:** Relatively small training sample (250 samples) **Right:** Relatively large sample. Results are averaged over 5 experimental runs

takes several days for a single evaluation using high performance computing), emulating the computer simulator with a machine learning model, known as surrogate model, that can be evaluated quickly can be a valuable approach (see [Chen and Hobson, 2019] for methods to statistically infer parameters using surrogate models). Training a model to accurately emulate a simulator is a supervised learning task and an application in which gradient information can be useful as it can be straightforward to extract the required gradient information (see [Brehmer *et al.*, 2020] for further discussion).

This example adapts the 2-dimensional dynamic toy problem from [Chen and Hobson, 2019]. The true simulator function is shown in Equation 7.

$$y_t = (\cos[\phi(\theta_1 - t - \alpha)] \cos[\phi(\theta_2 - t - \alpha)])^2 \quad (7)$$

The latent parameter set is $\theta = [\theta_1, \theta_2]$ and other parameters are set $\phi = 0.1$ and $\alpha = 5$. t represents the time step of the simulator and ranges from $T = [1, 2, \dots, 9, 10]$. Latent parameter input dimensionality is $J = 2$ and output dimensionality is $M = 1$.

To emulate the true function a feed forward neural network is used, implemented in Python using Keras (TensorFlow backend) [Chollet and others, 2015]. Note that the underlying function is not computationally expensive to evaluate for this example which allows surrogate model accuracy to be evaluated against true simulator outputs. Gradients from the true function are extracted using automatic differentiation via the autograd library in Python [Maclaurin D and others, 2014]. These gradients are then fit to the derivative output of the neural network with respect to inputs (automatically computed by Keras) using mean-squared error loss. The full objective function is a composite of surrogate output to target

loss and surrogate gradient to target gradient loss shown in Equation 8.

$$\min_{\varphi} L_t = 0.5(\mathbf{y}_t - \hat{\mathbf{y}}_t)^2 + 0.5(\nabla_{\theta} \mathbf{y}_t - \nabla_{\theta} \hat{\mathbf{y}}_t)^2 \quad (8)$$

where $\hat{\mathbf{y}}_t = \hat{s}_{\varphi,t}(\theta)$

Where both \mathbf{y}_t and $\hat{\mathbf{y}}_t$ have dimensionality $M \times 1$ for a simulator with M outputs at each time step t .

Model accuracy is evaluated over a range of neural network complexities. Models are comprised of an input layer with J nodes if $t = 1$, otherwise $(J + M)$ where J is the latent parameter dimensionality, 4 hidden layers each with $4 \times \eta$ nodes and an output layer with M nodes. Each hidden layer has a hyperbolic tangent activation function and the output layer has a linear activation function. Models are trained for 300 epochs with a time based learning rate decay that begins at 0.01 and approaches 0.0005 at epoch 300.

Surrogate model accuracy is also evaluated over a range of training sample sizes, tuned using trial and error to provide an informative sample range.

Neural network training and maximum likelihood estimation was performed on Google Colab servers using Tensor Processing Units (TPUs).

Latent parameter samples used for surrogate training are drawn from a uniform prior over the interval $\theta \sim U_{[0,15]}$. These samples are then run through the simulator and gradients are extracted to generate a training data set $\{\theta_i, \mathbf{y}_i, \nabla_{\theta} \mathbf{y}_i\}_{i=1}^N$ where $\mathbf{y}_i = [y_1, y_2, \dots, y_9, y_{10}]$. The performance of surrogate networks trained with and without gradients over a range of training sample sizes N and model complexities is presented in Figure 2.

Experimental results show three notable features:

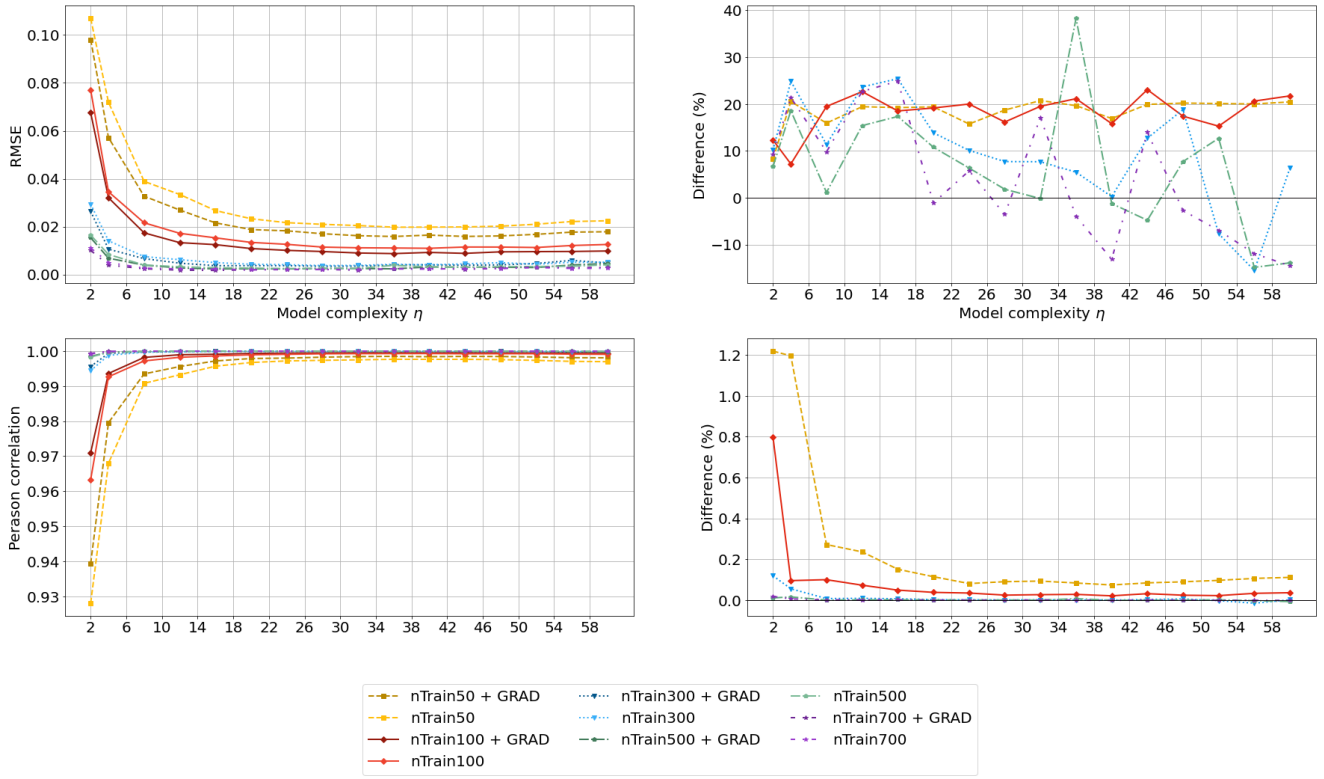


Figure 2: 2D problem surrogate model test accuracy. RMSE left/Pearson correlation (right) of surrogates models prediction on 1000 test data samples. Surrogates are trained on varying training sample sizes with varying complexities and either with (darker colours) or without (lighter colours) gradients. Model complexity values η correspond to a neural network with 4 hidden layers, each with $\eta * 4$ nodes. Results are averaged over 10 random draws from a fixed pool of 1000 synthetic training data points generated by the cosine function. Axes are set to emphasises region of interest.

1. Gradient trained surrogates consistently outperform conventionally trained surrogates when the training sample size is small; and
2. Gradient trained surrogates consistently outperform conventionally trained surrogates when the surrogate model complexity is low; and
3. Gradient trained surrogates outperformance deteriorates and becomes unstable for large sample sizes and high model complexities.

Each of these three features is discussed in detail below, however the results at a high level are intuitive: the marginal benefit of the information that gradients provide for training a model is largest when information is scarce (small training sizes). Therefore increasing training sample size reduces the value of the additional information gradients provide.

Note that the terms used here (e.g. small sample, high complexity) are relative to the underlying 2-dimensional process. When generalising these insights, whether or not a training data set is large or small or a model is simple or complex must also be considered relative to the underlying process of interest. The relationship is intuitive, more complex underlying processes require more training data and more complex surrogates in order to allow the surrogate to capture these complexities. A large amount of data for a simple 1-dimensional

linear underlying process could therefore be a small amount of data for a higher dimensional and/or non-linear process.

1. Small sample performance

Classical machine learning model (linear regression, neural network, regression forest, k-means, etc.) prediction on test data can be characterised as varying forms of interpolation between training data points. Accurate prediction on unseen data therefore requires large amounts of training data in order to sufficiently cover the possible input/output relationship across the entire input space. This is well understood and typically motivates efforts to train models on large amounts of data (often as much as possible given availability and computational constraints).

Framed this way, it becomes clear that prediction on test data is poorest when a model has seen only a small amount of training data as it cannot effectively generalise the learned relationship for data in unseen input regions. The gap between the models learned parameters and the mechanism underpinning the true process of interest is therefore largest when training data is scarce and so there is the greatest opportunity for extra information to close this gap and improve model fit. Gradients provide this extra information and help correct model parameters. Naturally this correction benefits parameters when they are most incorrect, which occurs when training samples sizes are small.

Inference problems that involve computationally expensive simulators are typically candidates for surrogate models in order to avoid requiring multiple simulator runs during the inference process. It follows that training data sets for these problems are likely to be relatively scarce for the same reason: simulator runs which generate training data are costly. The outperformance of the gradient trained surrogates is therefore largest for inference problems where surrogates may be the natural choice.

2. Low model complexity performance

The relationship between surrogate model complexity and gradient outperformance is clear however the reasons behind it are less so. One possible explanation is that just as small training samples create models that generalise to unseen data poorly, low complexity models (those with relatively few nodes) are similarly unable to generalise to unseen data and therefore benefit most from the correction that gradient information provides.

Generally simplistic models may be preferable to complex models for both practicable reasons (model training time) and philosophical reasons (Ockhams’s razor) and therefore adding gradients to surrogate training may be particularly desirable when a practitioner has a preference for simple models. The overarching goal of a practitioner is to choose a surrogate model that provides the most accurate emulation of the simulator however, and therefore the benefits of faster model training must be considered against potentially poorer surrogate accuracy. Leveraging gradients in surrogate training can help boost the performance of low complexity surrogates which potentially makes them a more desirable choice than more complex models with similar accuracy.

3. Large sample, high complexity performance

When training sample sizes are large and model complexity is high the performance of gradient trained surrogates relative to conventionally trained surrogates is unstable. This follows as the inverse consequence of the prior two results. When the training size is large there is little additional benefit that can be obtained by including gradients to model fitting. With a large training sample there is already enough ‘information’ in the training data to accurately emulate the underlying simulator and adding gradients has no benefit.

Note that this result does not appear to be a consequence of complex models over-fitting to training data as shown in the Appendix A.2 as train and test accuracy of the surrogates are not significantly different.

To demonstrate methods that employ surrogate models for latent parameter inference and show the effect more accurate surrogate models can have, maximum likelihood estimation is performed using optimal surrogate models for each training sample size. The likelihood draws from [Chen and Hobson, 2019], shown in Equation 9.

$$P(D_o|\theta^{(i)}) = \prod_{n=1}^N \prod_{t=1}^T \prod_{m=1}^M \left\{ \frac{1}{\sqrt{2\pi\sigma_{t,m}^2}} \exp \left[\frac{-(d_{t,m} - y_{t,m}^{(i)})^2}{2\sigma_{t,m}^2} \right] \right\} \quad (9)$$

$D_o = [\mathbf{d}_1, \mathbf{d}_2, \dots, \mathbf{d}_{T-1}, \mathbf{d}_T]^T$ where \mathbf{d} has dimensionality $M \times 1$ and represents observed (true) data from the process

and $y_{t,m}$ are synthetic outputs given inputs θ , which can be replaced with $\hat{y}_{t,m}$ from a surrogate model. N represents the size of the observed data sample and $\sigma_{t,m}^2$ is an estimate of the noise present in the true observations.

10 observations are generated from the true process (equation 7) with Gaussian noise $\epsilon \sim N(0, 0.001)$ added and so $\sigma_{t,m}^2 = 0.001$ to mirror to noise in the observation data. The true latent parameters are set to $\theta = [\theta_1, \theta_2] = [5, 5]$. Optimal surrogate model complexities are used for each training sample size, defined as the complexity which produces the lowest RMSE on unseen data.

Figure 3 shows the absolute difference between the inferred parameters using maximum likelihood estimation under optimal surrogate models trained with and without gradients.

The gradient trained surrogate model is able to produce more accurate parameter estimates under MLE for sample sizes 50, 100 and 300. As the training sample size increase beyond this level, the difference between the surrogate trained with and without gradients becomes immaterial and so the gradient trained surrogate outperformance subsides.

4 Hyper-Parameter Tuning: Delta-Min

4.1 Deriving Delta-Min

A key feature of the results discussed in Section 3 is that for ‘large’ training sample sizes and ‘high’ model complexities, the out-performance of gradient trained model becomes unstable. This result motivates a novel method for determining an upper bound to neural network complexity, coined delta-min or δ_{min} , where complexity refers to the number of nodes in a feed-forward neural network.

Model complexity is an important hyper-parameter to optimise when designing neural networks for any supervised learning task, highlighted by the results in Section 3.

The assumptions behind the delta-min method are as follows: First consider an accuracy measure A to evaluate the performance of a model’s predictions. Root-mean squared error (RMSE) is a straightforward choice for regression problems although the following logic generalises for any accuracy measure. The RMSE of a neural network’s N predictions (\hat{y}) of true target variables (y) is shown in Equation 10.

$$A[\hat{y}] = \sqrt{\frac{(y - \hat{y})^2}{N}} \quad (10)$$

A neural network’s predictions can be expressed as a function of model complexity $\hat{y} = F_\varphi(\mathbf{X}, c)$ where c refers to the number of nodes within a neural network and \mathbf{X} refers to a input data.

Assumption 1: $\frac{\delta A}{\delta c} \in \mathbb{R}$ is a monotonic non-decreasing ² function of c .

Assumption 1 implies that there is some optimal model complexity c^* that produces the optimal accuracy measure

²The specific accuracy measure selected alters the specifics of this assumption. For an accuracy measure such as correlation then $\frac{\delta A}{\delta c}$ must be a monotonic non-increasing function as a more accurate model has a *higher* correlation to y (rather than a lower RMSE).

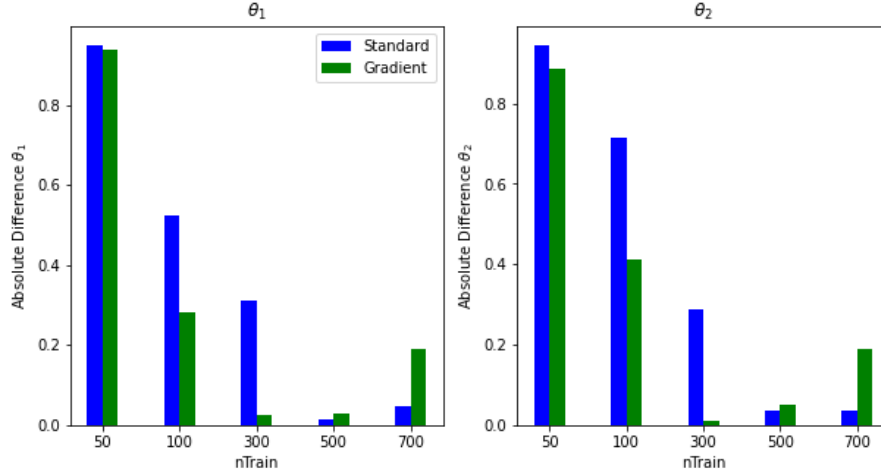


Figure 3: Absolute difference between latent parameters estimates using maximum likelihood with optimal surrogate models trained with and without gradients over varying sample sizes. Average of 10 surrogate models (each trained on random samples of training data for each sample size) is used for predicted values.

(e.g. lowest RMSE) A^* . Naturally, a practitioner designing neural network architecture seeks to find c^* .

A neural network trained with gradient information can be denoted as $F_\varphi^G(\mathbf{X}, c)$.

Assumption 2: For $c \leq c^*$: $A[F_\varphi^G(\mathbf{X}, c)] \leq A[F_\varphi(\mathbf{X}, c)]$ where A is RMSE (invert for accuracy measures that increase as predictions become more accurate, i.e correlation).

Assumption 2 implies that gradient information has value (improves model accuracy) when model complexity is *below* optimal which becomes evident from the results in Section 3.

Assumption 3: For $c \leq c^*$: $\nabla_c A[F_\varphi^G(\mathbf{X}, c)] \geq \nabla_c A[F_\varphi(\mathbf{X}, c)]$ where A is RMSE (invert for accuracy measures that increase as predictions become more accurate, i.e correlation).

Assumption 3 is the most restrictive and implies that when models have below optimal complexity, the improvement in accuracy that follows from increasing complexity (Assumption 1) is at least as large for models trained without gradients relative to those trained with. This requires that the value of gradient information for model training diminishes as a model approaches optimal (supported by results in Section 3). It can intuitively be understood as gradient information adding most value to neural network models when their complexity is less optimal and therefore the marginal benefit of training with gradient information is largest. This is explained in Section 2

Under these assumptions, the minimum absolute difference between the accuracy of neural networks trained with and without gradients can be used as an indicator of an upper bound to model complexity c^{UB} . This complexity can be found using the delta-min metric, shown in Equation 11.

$$\delta_{min} = \min_c |A[F_\varphi^G(\mathbf{X}, c)] - A[F_\varphi(\mathbf{X}, c)]| \quad (11)$$

To support these assumptions and the demonstrate how

they can be utilised to determine c^{UB} , δ_{min} is computed for the 2-dimensional presented in Section 2 and in addition a 4-dimensional and 8-dimensional linear and non-linear (respectively) toy functions are experimented with.

The 4-dimensional problem is a Generalised Autoregressive Conditional Heteroscedasticity (GARCH) model, originally introduced by [Bollerslev, 1986]. GARCH models are a popular volatility model for economic and financial time series data (for example see [French *et al.*, 1987] and [Franses and Van Dijk, 1996] for seminal work validating GARCH(1,1) models over long time periods). GARCH models extend the standard class of Autoregressive Conditional Heteroscedasticity (ARCH) models, originally introduced by [Engle, 1982], by defining a time series as a function of its prior realised values *and* its prior conditional variance. A GARCH(1,1) model forecasting next period volatility is shown in equation 12.

$$\sigma_{t+1}^2 = \omega + \alpha u_t^2 + \beta \sigma_t^2 \quad (12)$$

In order to add a dynamic component to the toy problem, volatility predictions in to future periods $t+h$ where $h \geq 2$ are computed where subsequent forecasts exploit the relationship $E_t[u_{t+1}^2] = \sigma_{t+1}^2$.

$$\begin{aligned} \sigma_{t+h}^2 &= \omega + \alpha E_t[u_{t+h-1}^2] + \beta E_t[\sigma_{t+h-1}^2] \text{ for } h \geq 2 \\ &= \omega + (\alpha + \beta) E_t[\sigma_{t+h-1}^2] \text{ for } h \geq 2 \end{aligned} \quad (13)$$

The neural network model must therefore capture the behaviour of the GARCH(1,1) process described in equations 12 and 13. The input parameter set for this example is $\theta = [\mu, \omega, \alpha, \beta]$ and all parameters are drawn from an uniform prior $\theta \sim U_{[0,1]}$ and run through a GARCH(1,1) process to generate synthetic target data and gradient information. u_t and σ_t^2 are assumed to be known at time t .

A forecast window of $t+h$ for $h \in [1, 2, 3, 4, 5]$ is considered (e.g. volatility is forecasted up to 5 days in the future).

Neural networks modelling the 4-dimensional function use 4 hidden layers, each with $\eta \times 4$ nodes with hyperbolic tangent activation functions and a soft-plus activation function for the output layer constraining outputs to be positive and avoiding dead neurons issues associated with ReLU [Goodfellow *et al.*, 2016]. Hidden layers use the hyperbolic tangent activation function.

The 8-dimensional function is shown in Equation 14.

$$y = \beta_1 \mathbf{x}_0 + \beta_2 (\beta_3 \exp [\beta_4 (\mathbf{x}_1 - \alpha)]) + \beta_5 (\beta_6 \exp [\beta_7 (\mathbf{x}_2 - \eta)]) + \beta_8 \quad (14)$$

Where $\alpha = 0.1$ and $\eta = 0.2$. $\mathbf{X} = [\mathbf{x}_0, \mathbf{x}_1, \mathbf{x}_2]$ represents input data with 2 features and a constant. To generate training data for the neural network to train with, parameters $\beta = \{\beta_j\}_{j=1}^8$ are drawn from $\beta \sim U_{[-0.5, 0.5]}$ and input data is drawn from $\mathbf{X} \sim U_{[0, 1]}$.

Neural networks emulating the 8-dimensional function use 10 hidden layers, each with $\eta \times 4$ nodes. Hyperbolic tangent activation functions are used in the hidden layers and a linear output layer activation function is used. Models are trained for 300 epochs with a time based learning rate decay.

Neural network training was performed on Google Colab servers using Tensor Processing Units (TPUs).

The upper-bounds implied using the delta-min method for each example problem are presented in Table 1. Results show that the optimal model complexity, defined as the complexity which minimises model RMSE on unseen data for each training sample size consistently lies below the delta-min upper bound.

Problem	Training size	Optimal model	δ_{min} UB
2D	50	36	40
	100	40	52
	300	28	52
	500	24	32
	700	20	24
4D	100	10	46
	300	6	22
	500	6	18
	700	6	14
8D	2500	30	30
	5000	20	20
	7500	30	30
	10000	20	70

Table 1: Optimal model complexities (defined as complexity that produces lowest RMSE on unseen data) compared to the complexity upper-bound implied by the delta-min metric.

4.2 Genetic Algorithms

The proposed value of the delta-min upper bound is that it should allow a practitioner to rule out large model complexities, that are the most computationally expensive to train, early on in a hyper parameter optimisation pipeline. Genetic algorithms [Mitchell, 1995], so called because they incorporate biological phenomena such as random mutation and survival of the fittest, are a class of automatic optimisation methods that have become increasingly popular in recent years and natural application for the delta-min metric.

Figure 4 demonstrates an example automatic hyper parameter optimisation pipeline that incorporates the δ_{min} metric to evaluate model complexity.

Model complexities above the complexity implied by δ_{min} can be ruled out in early iterations of the algorithm allowing for more efficient evaluation of granular hyper-parameter values in subsequent runs. Conducting experiments validating the utility of the δ_{min} metric for hyper-parameter optimisation using genetic algorithms is a recommended area for future research.

5 Ridge-Gradients Regularisation

To demonstrate the value of gradients for improving linear regression model fit this work presents a novel regularisation method coined Ridge-Gradients regularisation. The method builds upon Ridge regularisation, a well known modification to ordinary least squares (OLS) linear regression originally proposed by [Hoerl and Kennard, 1970] that penalises large coefficient values. Regularised linear models often outperform non-regularised equivalents as large coefficient values are typically a feature of models which have overfit to training data sets and therefore generalise poorly to unseen data.

The Ridge-Gradients optimisation problem is defined as:

$$\min_{\beta_{rg}} (\mathbf{z} - \hat{\mathbf{z}})^2 + \lambda_1 \hat{\beta}_{rg}^2 + \lambda_2 (\hat{\beta}_{rg} - \hat{\beta}_{grad})^2 \quad (15)$$

This optimisation problem includes the conventional goal of minimising the difference between model predictions $\hat{\mathbf{z}}$ and true process outputs \mathbf{z} and penalises large coefficient values with the standard Ridge shrinkage parameter $\lambda_1 \geq 0$. Gradients are leveraged in the third term which involves penalising, using $\lambda_2 \geq 0$, the difference between the coefficient $\hat{\beta}_{rg}$ and a new quantity, $\hat{\beta}_{grad}$. $\hat{\beta}_{grad}$ is the coefficient vector calculated using OLS with Ridge regularisation that fits *derivative inputs* to output gradients $\frac{\partial \mathbf{z}}{\partial \mathbf{x}}$.

To understand $\hat{\beta}_{grad}$, consider the following example where the true process is $P(\mathbf{x}) = \sin \mathbf{x}$ and \mathbf{x} is 1-dimensional input vector over the interval $[0, 2\pi]$. To fit a linear model to a non-linear sine wave the 1-dimensional input vector \mathbf{x} can be projected to higher dimensional space using radial basis functions (RBF) with evenly spaced centres in the input interval. This is illustrated in Figure 5 and the RBF equation is shown in Equation 16. The resulting input matrix is denoted $\Phi(\mathbf{x})$ and has dimensionality $N \times (C + 1)$ where N is the size of the training sample and C is the number of basis functions used plus a constant term. This example proceeds with $C = 7$ basis functions as this is sufficient to fit a sine curve reasonably well³.

$$\Phi_i(\mathbf{x}) = \exp \left\{ \frac{-(\mathbf{x} - c_i)^2}{r^2} \right\} \quad (16)$$

³The exact number of basis functions does not effect the key results and was determined via trial and error. See [Tipping and Faul, 2003] for automatic methods to optimally determine this quantity.

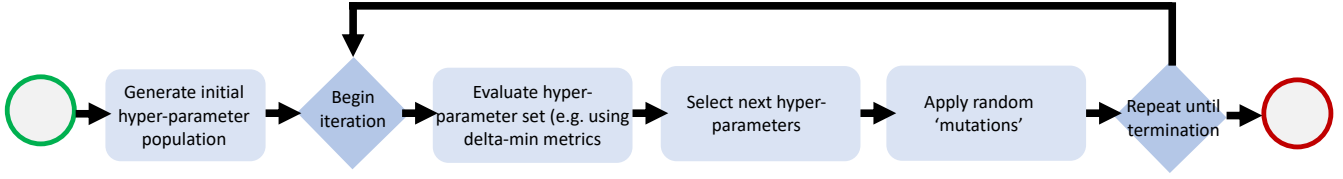


Figure 4: Genetic algorithm optimisation procedure incorporating δ_{min} metric.

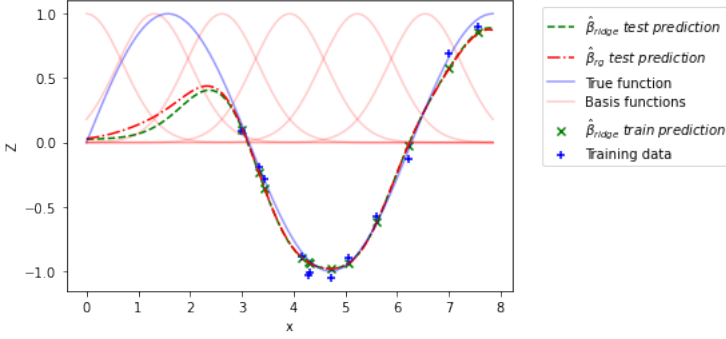


Figure 5: OLS model predictions of sine wave using 12 training data samples and 7 evenly distributed basis functions with $r=1$ (and a constant). $\hat{\beta}_{ridge}$ is calculated using OLS with Ridge regularisation with $\lambda_1 = 0.1$ optimised using a validation data set. $\hat{\beta}_{rg}$ is calculated using OLS with Ridge-Gradients regularisation with $\lambda_1 = 0.1$ and $\lambda_2 = 0.1$ optimised using a validation data set. Test RMSE of $\hat{\beta}_{rg}$ and $\hat{\beta}_{ridge}$ is 0.31 and 0.35 respectively (compared to a standard deviation of the test output data of 0.69)

The linear model with coefficients $\hat{\beta}_{ridge} = [\hat{\beta}_{0ridge}, \hat{\beta}_{1ridge}, \dots, \hat{\beta}_{7ridge}]^T$ fit using OLS with ridge regularisation is:

$$\hat{\mathbf{z}} = \hat{\beta}_{ridge} \Phi(\mathbf{x}) = \hat{\beta}_{0ridge} + \dots + \hat{\beta}_{1ridge} \exp\left\{\frac{-(\mathbf{x} - c_1)^2}{r^2}\right\} + \hat{\beta}_{7ridge} \exp\left\{\frac{-(\mathbf{x} - c_7)^2}{r^2}\right\} \quad (17)$$

In this example both necessary conditions required to leverage gradient information are satisfied as the derivative of \mathbf{z} with respect to \mathbf{x} is easily calculated and a linear regression output $\hat{\mathbf{z}}$ is differentiable with respect to its inputs \mathbf{x} . After calculating and retaining $\frac{\delta \mathbf{z}}{\delta \mathbf{x}}$, OLS (again with ridge regularisation) can be used to calculate $\hat{\beta}_{grad} = [\hat{\beta}_{0grad}, \hat{\beta}_{1grad}, \dots, \hat{\beta}_{7grad}]^T$, training the derivative inputs to the derivative outputs. The resulting 'gradient' fitting model takes the form:

$$\frac{\delta \hat{\mathbf{z}}}{\delta \mathbf{x}} = \hat{\beta}_{0grad} + \hat{\beta}_{1grad} \frac{-2(\mathbf{x} - c_1)^2}{r^2} \exp\left\{\frac{-(\mathbf{x} - c_1)^2}{r^2}\right\} + \dots + \hat{\beta}_{7grad} \frac{-2(\mathbf{x} - c_7)^2}{r^2} \exp\left\{\frac{-(\mathbf{x} - c_7)^2}{r^2}\right\} \quad (18)$$

The derivative of original OLS model from Equation 17 with respect to inputs can also be calculated to obtain:

$$\frac{\delta \hat{\mathbf{z}}}{\delta \mathbf{x}} = \hat{\beta}_{0ridge} + \hat{\beta}_{1ridge} \frac{-2(\mathbf{x} - c_1)^2}{r^2} \exp\left\{\frac{-(\mathbf{x} - c_1)^2}{r^2}\right\} + \dots + \hat{\beta}_{7ridge} \frac{-2(\mathbf{x} - c_7)^2}{r^2} \exp\left\{\frac{-(\mathbf{x} - c_7)^2}{r^2}\right\} \quad (19)$$

The key difference between $\hat{\beta}_{grad}$ and $\hat{\beta}_{ridge}$ is that $\hat{\beta}_{grad}$ is fit using OLS with the gradients of outputs with respect to inputs $\frac{\delta \mathbf{z}}{\delta \mathbf{x}}$ as the target variable. Naturally this means $\hat{\beta}_{grad}$ will be a better predictor of the true gradients of the underlying function than $\hat{\beta}_{ridge}$. This is confirmed and illustrated in Figure 6.

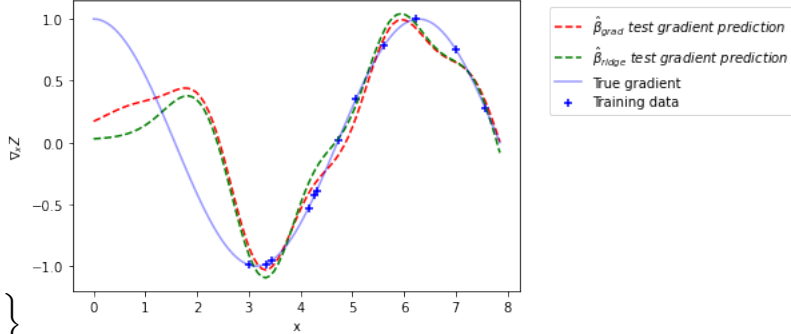


Figure 6: Predictions of the gradient of the sine wave using $\hat{\beta}_{grad}$ and $\hat{\beta}_{ridge}$. The RMSE using $\hat{\beta}_{ridge}$ is 0.4 and the RMSE using $\hat{\beta}_{grad}$ is 0.37.

From Equations 18 and 19 it becomes clear that in an optimal model there would be no difference between $\hat{\beta}_{grad}$ and $\hat{\beta}_{ridge}$ in order to optimally predict $\frac{\delta \mathbf{z}}{\delta \mathbf{x}}$. The goal of the additional regularisation term shown in Equation 15 is therefore to penalise differences between the coefficient vector fit to the target variable and the coefficient vector that optimally fits the target's gradients as in an optimal model, both should be fit well.

$$\hat{\beta}_{rg} = (\Phi' \Phi + \lambda_1 \mathbf{I} + \lambda_2 \mathbf{I})^{-1} (\lambda_2 \hat{\beta}_{grad} + \Phi' \mathbf{Z}) \quad (20)$$

The Ridge-Gradient (RG) solution, shown in Equation 20, can be calculated as (full derivation shown in Appendix A.1):

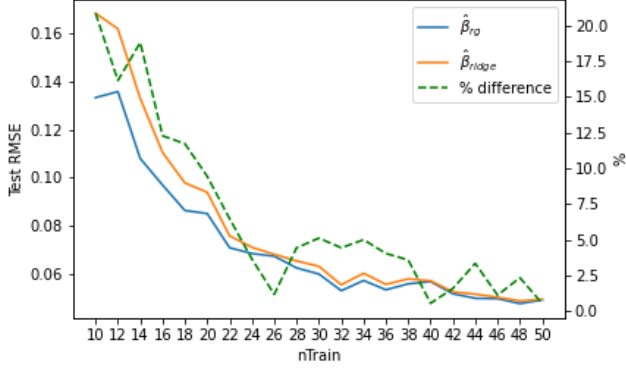


Figure 7: Comparative performance of $\hat{\beta}_{ridge}$ and $\hat{\beta}_{rg}$ over 50 random samples of training data of sizes in intervals of 2 from 10 to 50. Positive percentage difference indicates $\hat{\beta}_{rg}$ outperforms.

This regularisation method consistently outperforms vanilla Ridge regularisation over a range of training samples and sizes, as shown in Figure 7.

6 Training GANs with gradient information

Gradient information can be used to train Generative Adversarial Networks (GANs) [Goodfellow *et al.*, 2014]. GANs are deep neural net architectures that are typically composed of a pair of competing neural networks: a generator and a discriminator. The models are trained by alternately optimizing two objective functions so that the generator G learns to produce samples resembling real images, and the discriminator D learns to better discriminate between real and fake data.

Training GANs with gradients requires minor modifications to the conventional GAN training procedure. First, two discriminators are used (rather than one) to facilitate the mechanics of gradient training. One discriminator is conventional in that it aims to classify images as real or fake without using gradient information. Each iteration however, the conventional discriminator passes its updated parameters to a gradient discriminator. The gradient discriminator then trains the generator to produce images that it not only classifies as real, but also give 'real' derivatives of outputs with respect to inputs. The full algorithmic procedure is shown in Algorithm 1 and illustrated in Figure 8.

The procedure is best understood as the conventional GAN training procedure where the generator network G is trained to emulate not only the 'real' outputs according to a discriminator, but also the derivative of 'real' outputs with respect to 'real' inputs.

To demonstrate the value of gradient information for training GANs, basic GAN code is adapted to leverage gradient information for generating hand written digit images from the MNIST data set [Deng, 2012]. To evaluate the relative performance of gradient trained GAN compared to a conventionally trained equivalent, two metrics are presented. First, the change in the accuracy of the conventional discriminator $D_{standard}$ is computed each training iteration. Each iteration, the generator network is trained to fool an improved discriminator. Therefore by comparing the change in the accuracy

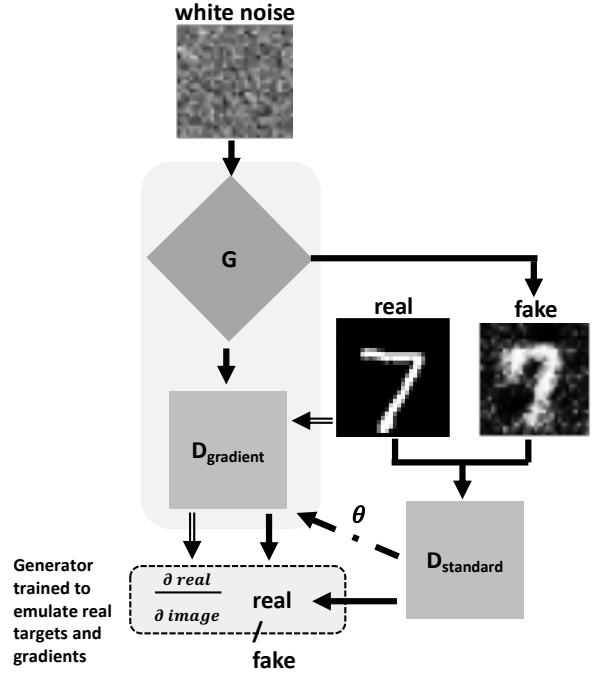


Figure 8: Architecture of gradient trained GAN.

Algorithm 1 Gradient trained GAN

Input: White noise and true images

Parameter: Epochs (number of parameter updates to train each network)

Output: Generated images

- 1: Initialise generator, conventional discriminator and gradient discriminator networks.
 - 2: **for** iteration **do**
 - 3: Generate fake images using generator network G .
 - 4: Generate and store derivatives of gradient discriminator $G_{gradient}$ with respect to real images inputs.
 - 5: Train conventional discriminator $D_{standard}$.
 - 6: Pass trained parameters to gradient discriminator $D_{gradient}$.
 - 7: Train generator to generated images that:
 1. Produces 'real' targets, according to $D_{gradient}$; and
 2. Produces 'real' gradients, according to $D_{gradient}$.
 - 8: **end for**
 - 9: **return** Generated images
-

of $D_{standard}$ that results before and after training the generator, the marginal change in image quality per epoch can be inferred. If the generator produces more realistic images each epoch, the accuracy of the discriminator will fall, which is indeed the case for the GANs under both training schemes, as shown in Figure 9.

The larger reduction in discriminator accuracy is greater per iteration under the gradient training scheme demonstrates the value of training generators with the gradient information.

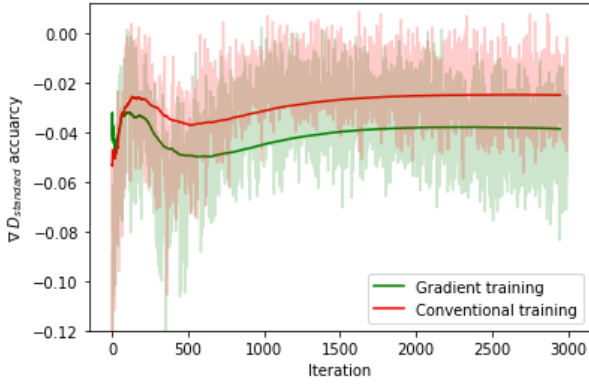


Figure 9: Decrease in conventional discriminator ($D_{standard}$ accuracy) per iteration when generator is trained with and without gradients. Rolling average is plotted with solid line. Results use average of 10 experimental trials.

Table 2 evaluates GANs that have undergone significant training (15,000 epochs) to compare the image quality of generative networks trained with and without gradient information. The Kullback–Leibler (KL) divergence and root mean-squared error (RMSE) are averaged for 150,000 images to give an objective indication of the quality of the images generated under each training scheme. The lower KL-divergence and RMSE of images generated under the gradient trained network indicate it is producing higher quality images.

Training scheme	KL-divergence	RMSE
Conventional	1022.130 ± 330.589	0.126 ± 0.032
Gradient	1004.036 ± 331.428	0.125 ± 0.032

Table 2: KL divergence and RMSE between 150,000 images generated via GANs trained for 15,000 epochs with and without (conventional) gradient information versus true images.

Under this relatively simple example, the difference between images generated under gradient and conventional trained networks does not appear discernible to the humans. As explained in Section 2, the value of gradient information is a function of a model’s error. One would therefore expect the apparent benefit of training networks with gradient information to be more readily apparent for comparatively more challenging (i.e. higher dimensional tasks).

7 Conclusion

This paper presents methods for leveraging gradient information to improve model prediction, focussing on applications for latent parameter estimation, linear regression regularisation, hyper-parameter tuning and generative models. The results demonstrate that the intrinsic gradient information extracted from the original model and the training data can be used to improve the performance of machine learning models. This approach is suitable for problems where the computer model (e.g., numerical simulators, generator networks in GAN) or mathematical expressions of the underlying (physical) process is known and differentiable. The pro-

posed method is particularly suitable for problems with very limited available training samples since the extracted gradient information can be viewed as extra training samples under certain conditions.

References

- [Blum *et al.*, 2013] M. G. B. Blum, M. A. Nunes, D. Prangle, and S. A. Sisson. A Comparative Review of Dimension Reduction Methods in Approximate Bayesian Computation. *Statistical Science*, 28(2):189 – 208, 2013.
- [Bollerslev, 1986] Tim Bollerslev. Generalized autoregressive conditional heteroskedasticity. *Journal of Econometrics*, 31(3):307–327, 1986.
- [Brehmer *et al.*, 2020] Johann Brehmer, Gilles Louppe, Juan Pavéz, and Kyle Cranmer. Mining gold from implicit models to improve likelihood-free inference. *Proceedings of the National Academy of Sciences*, 117(10):5242–5249, 2020.
- [Casciano *et al.*, 2015] C. Casciano, A. Cominelli, and M. Bianchi. Latest Advances In Simulation Technology For High-resolution Reservoir Models: Achievements And Opportunities For Improvement. volume Day 3 Wed, September 16, 2015 of *SPE Reservoir Characterisation and Simulation Conference and Exhibition*, 09 2015. D031S017R001.
- [Chen and Hobson, 2019] Xi Chen and Mike Hobson. Bayesian surrogate learning in dynamic simulator-based regression problems, 2019.
- [Chollet and others, 2015] Francois Chollet et al. Keras, 2015.
- [Deng, 2012] Li Deng. The mnist database of handwritten digit images for machine learning research. *IEEE Signal Processing Magazine*, 29(6):141–142, 2012.
- [Engle, 1982] Robert F. Engle. Autoregressive conditional heteroscedasticity with estimates of the variance of united kingdom inflation. *Econometrica*, 50(4):987–1007, 1982.
- [Franses and Van Dijk, 1996] Philip Hans Franses and Dick Van Dijk. Forecasting stock market volatility using (non-linear) garch models. *Journal of Forecasting*, 15(3):229–235, 1996.
- [French *et al.*, 1987] Kenneth R. French, G. William Schwert, and Robert F. Stambaugh. Expected stock returns and volatility. *Journal of Financial Economics*, 19(1):3–29, 1987.
- [Goodfellow *et al.*, 2014] Ian J. Goodfellow, Jean Pouget-Abadie, Mehdi Mirza, Bing Xu, David Warde-Farley, Sherjil Ozair, Aaron Courville, and Yoshua Bengio. Generative adversarial networks, 2014.
- [Goodfellow *et al.*, 2016] Ian Goodfellow, Yoshua Bengio, and Aaron Courville. *Deep learning*. MIT press, 2016.
- [Gutmann *et al.*, 2018] Michael U Gutmann, Ritabrata Dutta, Samuel Kaski, and Jukka Corander. Likelihood-free inference via classification. *Statistics and Computing*, 28(2):411–425, 2018.

- [Hoerl and Kennard, 1970] Arthur E Hoerl and Robert W Kennard. Ridge regression: Biased estimation for nonorthogonal problems. *Technometrics*, 12(1):55–67, 1970.
- [Maclaurin D and others, 2014] Johnson M Maclaurin D, Duvenaud D et al. autograd, 2014.
- [Mitchell, 1995] Melanie Mitchell. Genetic algorithms: An overview. In *Complex.*, volume 1, pages 31–39. Citeseer, 1995.
- [Papamakarios and Murray, 2016] George Papamakarios and Iain Murray. Fast epsilon-free inference of simulation models with bayesian conditional density estimation. In D. Lee, M. Sugiyama, U. Luxburg, I. Guyon, and R. Garnett, editors, *Advances in Neural Information Processing Systems*, volume 29. Curran Associates, Inc., 2016.
- [Rubin, 1984] Donald B. Rubin. Bayesianly Justifiable and Relevant Frequency Calculations for the Applied Statistician. *The Annals of Statistics*, 12(4):1151 – 1172, 1984.
- [Thomas *et al.*, 2016] Owen Thomas, Ritabrata Dutta, Jukka Corander, Samuel Kaski, and Michael U. Gutmann. Likelihood-free inference by ratio estimation, 2016.
- [Tipping and Faul, 2003] Michael E Tipping and Anita C Faul. Fast marginal likelihood maximisation for sparse bayesian models. In *International workshop on artificial intelligence and statistics*, pages 276–283. PMLR, 2003.
- [Tran *et al.*, 2017] Dustin Tran, Rajesh Ranganath, and David M Blei. Hierarchical implicit models and likelihood-free variational inference. In *Proceedings of the 31st International Conference on Neural Information Processing Systems*, pages 5529–5539, 2017.
- [van den Oord *et al.*, 2016] Aaron van den Oord, Nal Kalchbrenner, and Koray Kavukcuoglu. Pixel recurrent neural networks, 2016.

A Appendix

A.1 Ridge-Gradients Derivation

This appendix provides the derivation of the Ridge-Gradients coefficient shown in Equation 10 from Section 3.1. Transposed matrices and vectors denoted with a superscript T , e.g \mathbf{z}^T and the identity matrix denoted \mathbf{I} .

The objective function is:

$$\min_{\hat{\beta}_{rg}} Obj = (\mathbf{z} - \hat{\mathbf{z}})^2 + \lambda_1 \hat{\beta}_{rg}^2 + \lambda_2 (\hat{\beta}_{rg} - \hat{\beta}_{grad})^2 \quad (21)$$

Let $\hat{\mathbf{z}} = \mathbf{X}\hat{\beta}_{rg}$ where \mathbf{X} is a matrix containing the independent variable data with dimensionality $N \times M$ and $\hat{\beta}_{rg}$ is the Ridge-Gradients coefficient vector with dimensionality $M \times 1$. The objective function can therefore be written as:

$$Obj = (\mathbf{z} - \mathbf{X}\hat{\beta}_{rg})^2 + \lambda_1 \hat{\beta}_{rg}^2 + \lambda_2 (\hat{\beta}_{rg} - \hat{\beta}_{grad})^2 \quad (22)$$

Expanding this:

$$\begin{aligned} Obj = & \mathbf{z}^T \mathbf{z} - \hat{\beta}_{rg}^T \mathbf{X}^T \mathbf{z} - \mathbf{z}^T \mathbf{X} \hat{\beta}_{rg} + \hat{\beta}_{rg}^T \mathbf{X}^T \mathbf{X} \hat{\beta}_{rg} \\ & + \lambda_1 \hat{\beta}_{rg}^T \hat{\beta}_{rg} + \lambda_2 \hat{\beta}_{rg}^T \hat{\beta}_{rg} - \lambda_2 \hat{\beta}_{rg}^T \hat{\beta}_{grad} \\ & - \lambda_2 \hat{\beta}_{grad}^T \hat{\beta}_{rg} + \lambda_2 \hat{\beta}_{grad}^T \hat{\beta}_{grad} \end{aligned} \quad (23)$$

This can be simplified to:

$$\begin{aligned} Obj = & \mathbf{z}^T \mathbf{z} - 2\mathbf{z}^T \mathbf{X} \hat{\beta}_{rg} + \hat{\beta}_{rg}^T \mathbf{X}^T \mathbf{X} \hat{\beta}_{rg} + \\ & \lambda_1 \hat{\beta}_{rg}^T \hat{\beta}_{rg} + \lambda_2 \hat{\beta}_{rg}^T \hat{\beta}_{rg} - 2\lambda_2 \hat{\beta}_{rg}^T \hat{\beta}_{grad} + \\ & \lambda_2 \hat{\beta}_{grad}^T \hat{\beta}_{grad} \end{aligned} \quad (24)$$

Taking to the derivative and imposing the necessary condition to minimise the objective function:

$$\begin{aligned} \frac{\delta Obj}{\delta \hat{\beta}_{rg}} = & -2\mathbf{X}^T \mathbf{z} + 2\mathbf{X}^T \mathbf{X} \hat{\beta}_{rg} + \\ & 2\lambda_1 \hat{\beta}_{rg} + 2\lambda_2 \hat{\beta}_{rg} - 2\lambda_2 \hat{\beta}_{grad} = 0 \end{aligned} \quad (25)$$

Which can be simplified to:

$$\begin{aligned} \frac{\delta Obj}{\delta \hat{\beta}_{rg}} = & -\mathbf{X}^T \mathbf{z} + \mathbf{X}^T \mathbf{X} \hat{\beta}_{rg} + \lambda_1 \hat{\beta}_{rg} + \\ & \lambda_2 \hat{\beta}_{rg} - \lambda_2 \hat{\beta}_{grad} = 0 \end{aligned} \quad (26)$$

Rearranging terms:

$$\hat{\beta}_{rg} (\mathbf{X}^T \mathbf{X} + \lambda_1 \mathbf{I} + \lambda_2 \mathbf{I}) = \lambda_2 \hat{\beta}_{grad} + \mathbf{X}^T \mathbf{z} \quad (27)$$

Therefore the solution for $\hat{\beta}_{rg}$ can be written as:

$$\hat{\beta}_{rg} = (\mathbf{X}^T \mathbf{X} + \lambda_1 \mathbf{I} + \lambda_2 \mathbf{I})^{-1} (\lambda_2 \hat{\beta}_{grad} + \mathbf{X}^T \mathbf{z}) \quad (28)$$

A.2 Over-fitting analysis

The training versus test RMSE of the surrogate models for varying sample sizes and model complexities are presented for the 2-dimensional, 4-dimensional and 8-dimensional problems. For all problems, surrogate models do not demonstrate signs of over fitting as performance on seen and unseen data is not materially different.

2D problem

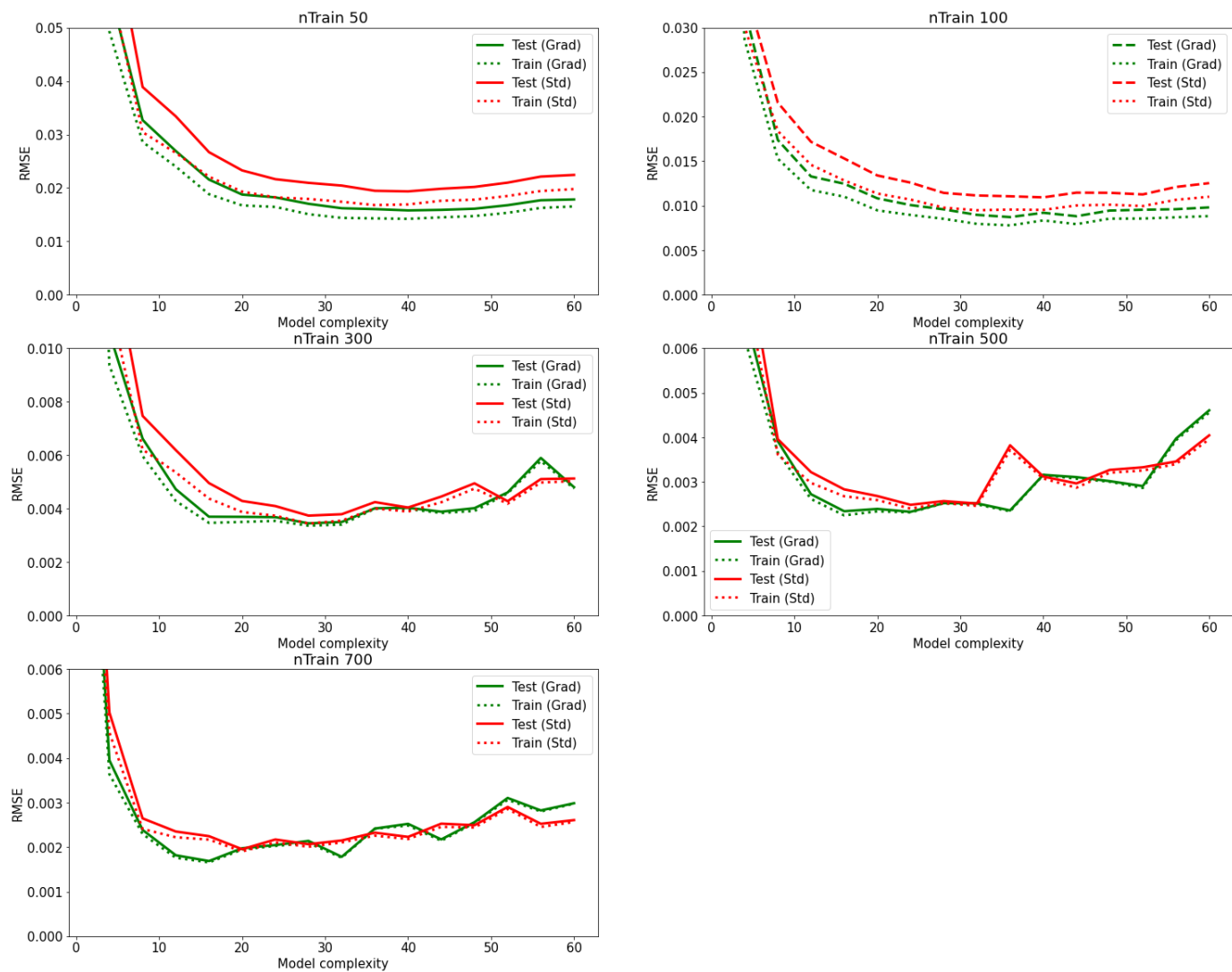


Figure 10: Train versus test RMSE for each surrogate model complexity and training sample size. Axes have been cropped to emphasis region on interest.

4D GARCH problem

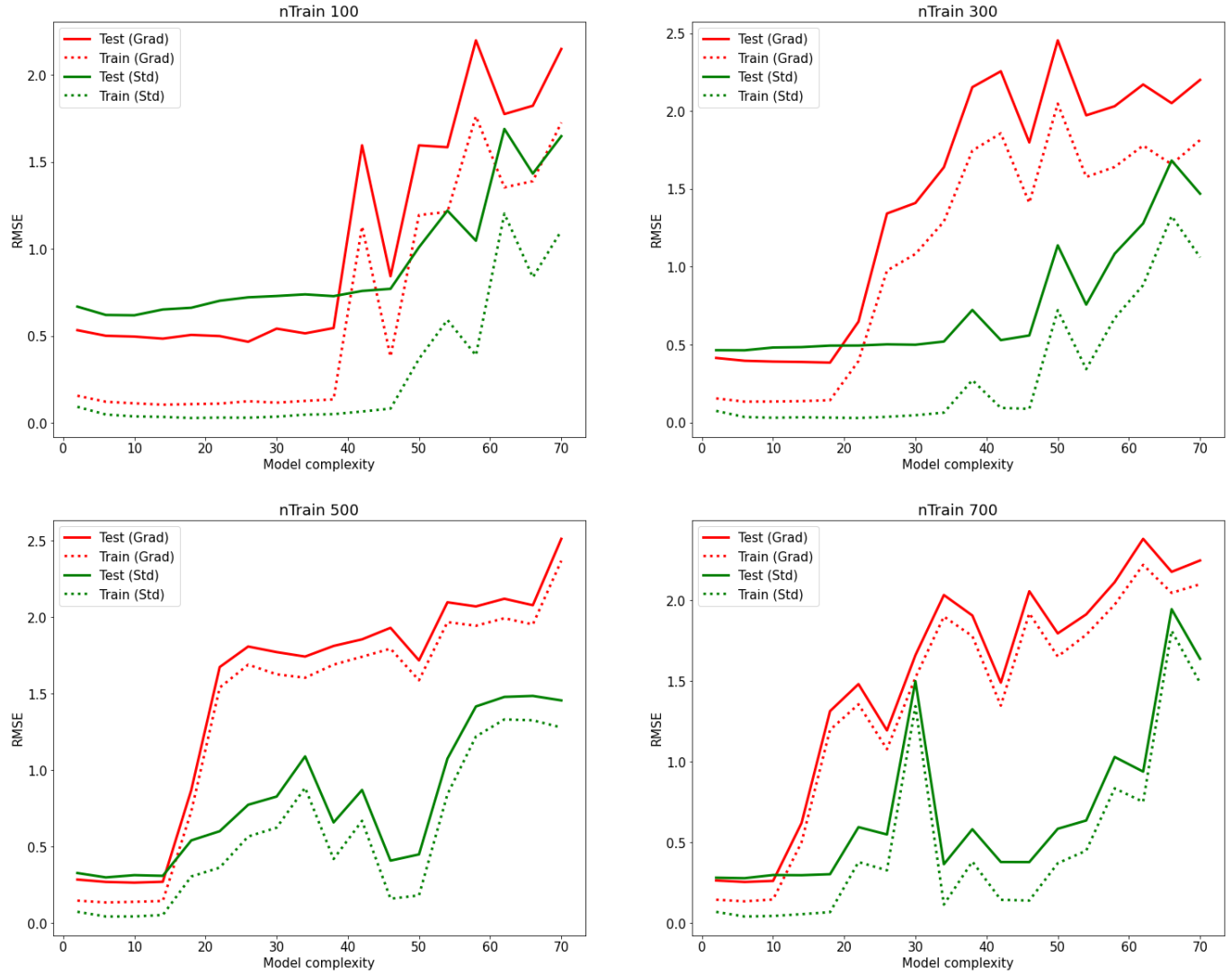


Figure 11: Train versus test RMSE for each surrogate model complexity and training sample size. Axes have been cropped to emphasis region on interest.

8D GARCH problem

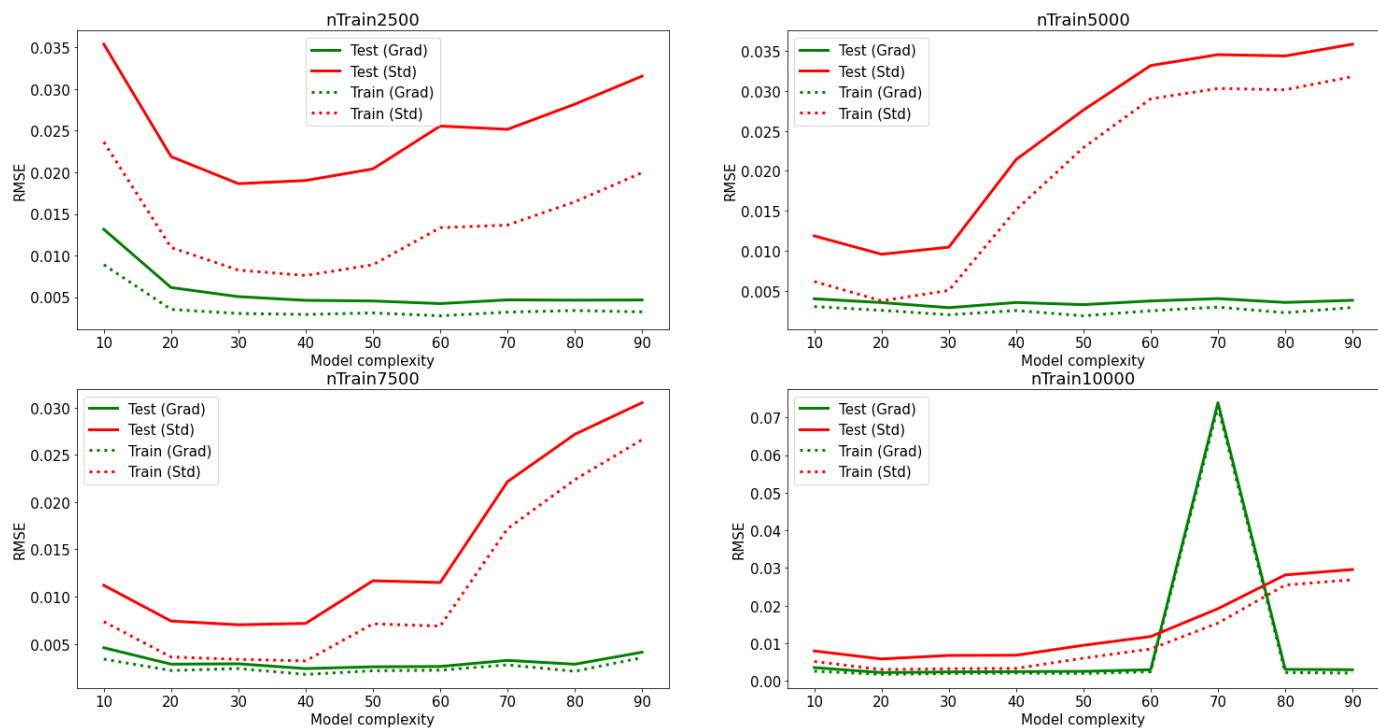


Figure 12: Train versus test RMSE for each surrogate model complexity and training sample size. Axes have been cropped to emphasize region on interest.